PROCEEDINGS OF ECOS 2023 - THE 36TH INTERNATIONAL CONFERENCE ON
EFFICIENCY, COST, OPTIMIZATION, SIMULATION AND ENVIRONMENTAL IMPACT OF ENERGY SYSTEMS
25-30 JUNE, 2023, LAS PALMAS DE GRAN CANARIA, SPAIN

Optimization of the pipe diameters and the dynamic operation of a district heating network

Malik Hakim Elhafaia[a], Arley Nova-Rincon[b], Sabine Sochard[c], Sylvain Serra[d] and Jean-Michel Reneaume[e]

[a,b,c,d,e] *Universite de Pau et des Pays de l'Adour, E2S UPPA, LaTEP, Pau, France*
[a] *malik-hakim.elhafaia@univ-pau.fr, CA,* [b] *arleynova@gmail.com,* [c] *sabine.sochard@univ-pau.fr,*
[d] *sylvain.serra@univ-pau.fr,* [e] *jean-michel.reneaume@univ-pau.fr*

Abstract:

In the research field of district heating networks (DHNs), there is a need for more analysis on the economic optimization of the design and dynamic operation considering precise representations of the temperature and pressure drops in the pipes of the system. In this study, we develop a model tested in an academic case study of a DHN composed of a production unit, a distribution network, and twenty consumers. The dynamic behavior of the DHN is due to the variability of the heat demand and ambient temperature over a daily period. Inside the pipes, the temperature variation is described by a dynamic one-dimensional heat transfer equation while the pressure drops are computed using the Darcy-Weisbach equation. Energy and mass balances are applied in the interconnecting nodes of the system. In addition, the model includes design and operational constraints of the DHN. All these equations lead to a partial differential algebraic equation (PDAE) problem. Using the method of orthogonal collocation on finite elements (OCFE), the differential terms are discretized to obtain a set of algebraic equations. The resulting non-linear programming (NLP) problem is solved with an equation-oriented (simultaneous) approach using the solver CONOPT. The aim of the optimization is to find the best trade-off between the capital expenditures (CAPEX) of the pipes and the operational expenditures (OPEX) by considering the pipe diameters, temporal values of mass flows and spatio-temporal values of temperatures of each pipe as continuous optimization variables. The CAPEX include the cost of the pipes and the cost of deploying them in trenches. The OPEX include both production and pumping costs which are related to thermal losses and pressure drops, respectively. As the pumping cost is significantly lower than the heat production cost, the results showed that it is more economical to reduce the thermal losses than the pressure drops.

Keywords:
District Heating Network; Dynamic optimization; Non-Linear Programming; Orthogonal Collocation on Finite Elements.

1. Introduction

Heating and cooling demand accounts for around half of global final energy consumption. Nearly half of this energy is used in industrial processes, 46% is used in residential and commercial buildings mainly for space and water heating. Most of the energy used for heating and cooling continues to be produced from non-renewable sources. Consequently, heating and cooling is responsible for 40% of energy-related greenhouse gas emissions [1]. The development of district heating and cooling (DHC) systems is a good answer to face these energy and environmental issues. This technology has the advantage of accelerating energy transition by integrating an important part of renewable sources and waste heat. Due to their considerable investment and operational costs, currently in the energy field, one of the important challenges is the development of tools and methods for the optimization of DHC networks.

According to how the time dependency is taken into account in the model, it is possible to classify the works on the optimization of DHC into four main categories: steady-state, quasi-steady-state, dynamic multi-period, and dynamic. In the steady state models, the optimization is performed with no time dependency considering averaged values for the operating parameters like mass flows and temperatures in the system. In most of the cases, the optimization problem is of the mixed integer programming type [2–4]. In [2] and [3] mixed integer linear programming (MILP) approaches are used for the optimizations of the operational cost and the total annual cost, respectively. Linear equations for the computation of thermal losses and pressure drops in the pipes are defined. In [4], the authors chose a mixed integer non-linear programming (MINLP) approach where the global cost of a district heating network (DHN) is optimized over 30 years. The thermal losses and pressure drops were computed with more precise equations. For the 3 previous studies, the discrete variables represent the design choices (connection in the topology nodes and/or the choices of production technologies). On the

 https://doi.org/10.52202/069564-0218

other hand, the continuous variables represent the operating parameters (production power, flows, temperatures, …). The authors of [5] opted for a non-linear programming (NLP) resolution where they used a numerical continuation strategy that gradually forces the design variables towards discrete choices. Steady-state models are interesting for long-term studies, but one of their main drawbacks is not considering a variable heat demand.

In what we classified as quasi-steady-state studies, it is possible to consider different values of the heat demand. The optimization is performed within a time interval which is subdivided into periods. For each period, the heat demand is averaged. The problem is a succession of steady-state problems. In this type of studies, Liu et al. [6] modeled an optimization of design parameters of a solar heating network. They took into account only discrete decision variables which were the network layout variables and pipe diameters. Sameti and Haghighat [7] studied the optimal design and operation of a DHN with a cogeneration unit. A MILP model was employed, and different buildings with different heat demands were considered. This kind of model is suitable for medium-term studies; however, it presents limits with dynamic aspects. As it does not include differential equations, for example, it is impossible to have the evolution of a thermal energy storage (TES) tank from one period to another.

In terms of time discretization, the studies we classify in the dynamic multi-period approach are quite similar to the previous category. The main difference is that they include at least one differential equation. In this category, Deng et al. [8] developed a MINLP model to perform what they called an optimal scheduling of a DHC. For each period, they define whether the technology is working or not, and the amount of power it produces (or charges/discharges in case of storage). Wirtz et al. [9] were also interested in the choice of technologies and the amount of produced and stored power of a DHC with multiple production technologies and TES. In addition, they optimized the temperature in the distribution network and the thermal losses. We have also Söderman [10] who optimized the topology and the operation to minimize the total annual cost of a district cooling network (DCN). He considered different consumers with different heat demands in each period. Another interesting study is the optimization of Khir and Haouari [11] of a DCN. They optimized chiller plant capacity, storage tank capacity, piping network size and layout, and produced and stored power during every period. In their operation, they ensure that supplied temperature corresponds to the desired one and that pressure drops are within the allowable limits. This type of works is suitable for medium-term studies with inclusion of dynamic aspects. In contrast, as they consider an important time step (≥ 1 hour), it is difficult to perform real-time control and/or to have precise evolutions of physical phenomena in the pipes.

What we chose to classify as dynamic approaches are the works that considered a small time step (<1 hour) and a short period of study (1-3 days generally). Two sub-categories can be distinguished, the studies that are for real-time optimization and the ones for dynamic offline optimization. In real-time models, Cox et al. [12] used a genetic algorithm to have the optimum control strategy of the operation of chillers and ice storage of a DCN. Lu et al. [13] developed a NLP optimization for the regulation of the operating parameters of a DHN. The limit with real-time models is that they require the calculation of the command in a short time. Therefore, they do not have precise thermo-hydraulic modeling of the pipes. This is where the interest of dynamic offline optimization (DOO) comes in with the possibility of having longer computation time; therefore, more accurate modeling of the pipes. In the DOO, Schweiger et al. [14] proposed a methodology to decompose a MINLP optimal control problem of a DHN into two sub-problems. A mixed problem to minimize the operational cost and a continuous one to minimize the production temperature. Nova Rincon et al. [15] studied another aspect of the optimal operation of a DCN. To avoid the technical issue of "Low ΔT syndrome" which reduces the efficiency of the system, they optimized the mass flows and temperatures in the distribution network to minimize the difference between the outlet temperature of consumers and a design outlet temperature. As they solve differential equations with a small time step, the DOO approaches have significant resolution times. To our knowledge, this is why we do not find studies that optimize at the same time the design and the dynamic operation of a DHC with accurate thermo-hydraulic modeling of the pipes. The originality of this work is that we conduct an optimization of the pipe diameters and the dynamic operation of a DHN with an economic objective function while having a precise modeling of the pipes.

In this study, we present a methodology for the optimal operation of an academic case study of a DHN comprised of twenty consumers over a daily study period. In addition to the optimization of mass flows and temperatures in the distribution network, the pipe diameters are also optimized. Considering a variable ambient temperature, a dynamic one-dimensional heat transfer equation is used to define the temperature evolution in the pipes. The Darcy-Weisbach equation is employed to compute the pressure drops in the distribution network. In the following parts, firstly we expose the case study. Secondly, we introduce the physical, the design and the operational constraints in addition to the objective function of the problem. Finally, we present the results and conclusions.

2. Case study

For this study, we used the same topology of the network presented in Figure 2 of [15] that serves 20 different consumers. In the outward path, there are 41 pipes, 21 main pipes $(0-20)$ and 20 lateral pipes $(in_1 - in_{20})$. The lateral pipes are directly connected to the consumers through a sub-station unit where the thermal power is transferred from the distribution network to the consumer's heating system. The return path is also comprised of 41 pipes that are parallel to the outward path ($0_r - 20_r$ and $out_1 - out_{20}$). The network is then constituted by 1 production unit, 20 substations and 82 pipes with a total length close to 19 km. In what follows, we use k as the index for all the pipes, p, p_r, in_p and out_p as the sub-indexes for main outward pipes, main return pipes, lateral pipes entering consumers and lateral pipes leaving consumers, respectively.

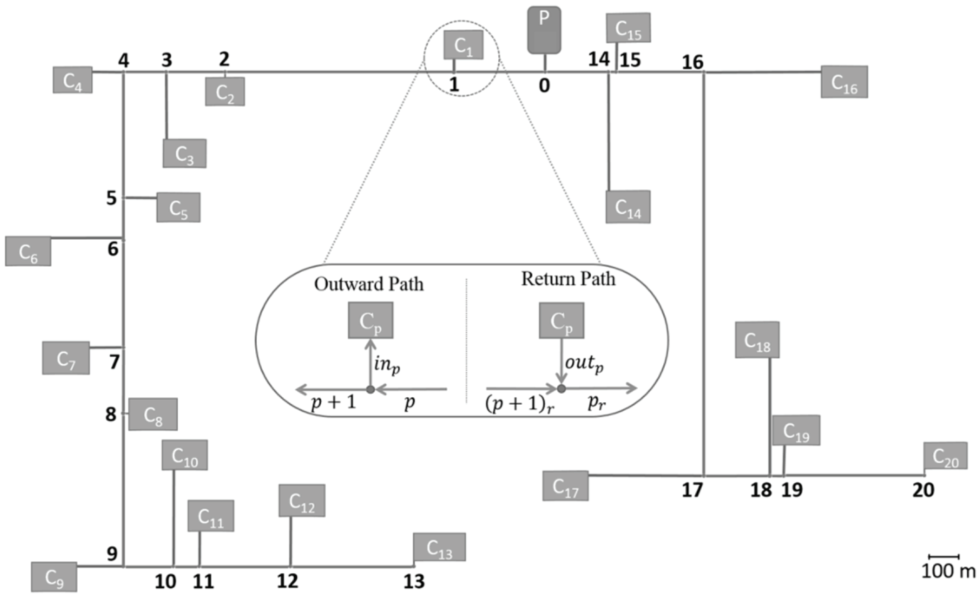

Figure 1. Representation of the network's configuration [15].

Concerning the heat demand, the same daily profiles used in district B of [16] are taking into account. Two types of profiles are considered, one for residential buildings, and one for commercial buildings. Table 1 shows the distribution of the type of buildings and their peak demand. The two profiles are represented as a function of the peak demand of each consumer as shown in Figure 2. To have a continuous representation of the two types of profile over time, a fit function was introduced for each profile. The two heat demand profiles of Figure 2 are defined by a sum of sinusoidal functions of the form:

$$Demand(t) = \sum_{i=1}^{8} \alpha_i \cdot \sin(\beta_i \cdot t + \gamma_i) \tag{1}$$

where α_i, β_i and γ_i are coefficients of the demand function.

Table 1. Type of consumers and their peak demands.

Consumer	Type	Peak demand	Consumer	Type	Peak demand
C_1	Commercial	1500	C_{11}	Commercial	720
C_2	Commercial	1260	C_{12}	Residential	180
C_3	Residential	360	C_{13}	Residential	450
C_4	Commercial	1440	C_{14}	Commercial	1500
C_5	Residential	210	C_{15}	Commercial	1050
C_6	Commercial	1020	C_{16}	Commercial	540
C_7	Residential	240	C_{17}	Commercial	990
C_8	Commercial	600	C_{18}	Commercial	1200
C_9	Commercial	990	C_{19}	Commercial	1170
C_{10}	Commercial	420	C_{20}	Commercial	1110

In Figure 3, the total heat demand of the network is represented. Its evolution is quite the same as the one of the commercial demand, because there are 15 commercial buildings in this case study and they have a higher peak demand than residential buildings. In the same figure, we also have the ambient temperature evolution which is one of a not very cold winter day.

3. System modeling

The model of the DHN is comprised of energy and mass conservation equations at each node and sub-station of the system. Inside every pipe, a heat transfer equation describes the temperature evolution. In this latter,

 https://doi.org/10.52202/069564-0218

the mass flow is time dependent, while the temperature is time and space dependent. In addition, the Darcy-Weisbach equation describes the dynamic evolution of pressure drops in the pipes. In the following parts, we will detail the different equations of the system. These equations represent the physical, design and operational constraints of the optimization problem.

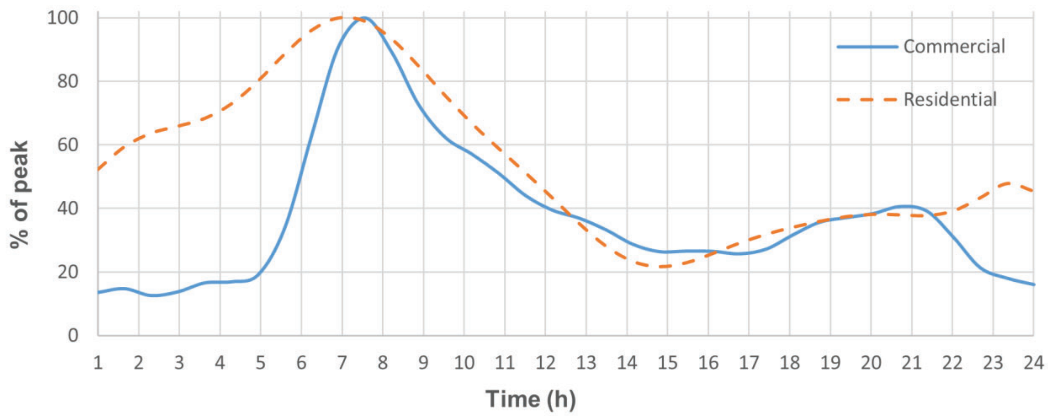

Figure 2. Heat demand profiles.

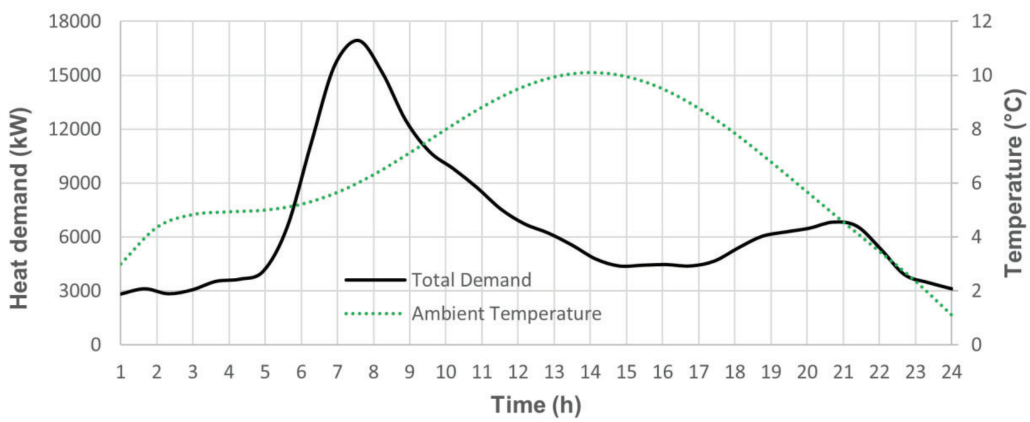

Figure 3. Total heat demand and ambient temperature profiles.

3.1. Production unit, nodes and sub-station

At the production level, we consider one fixed technology that delivers the hot water at a constant temperature:

$$T_{p=0}(t, x=0) = constant \tag{2}$$

At every interconnecting node of the network, the mass balance is applied. For the outward path, we have:

$$\begin{aligned} &\dot{m}_p(t) = \dot{m}_{p+1}(t) + \dot{m}_{in_p}(t) \quad p = 1 \dots 12, 14 \dots 19 \\ &\dot{m}_p(t) = \dot{m}_{in_p}(t) \quad p = 13, 20 \\ &\dot{m}_0(t) = \dot{m}_1(t) + \dot{m}_{14}(t) \end{aligned} \tag{3}$$

For the return path, we have:

$$\begin{aligned} &\dot{m}_{p_r}(t) = \dot{m}_{(p+1)_r}(t) + \dot{m}_{out_p}(t) \quad p = 1 \dots 12, 14 \dots 19 \\ &\dot{m}_{p_r}(t) = \dot{m}_{out_p}(t) \quad p = 13, 20 \\ &\dot{m}_{0_r}(t) = \dot{m}_{1_r}(t) + \dot{m}_{14_r}(t) \end{aligned} \tag{3}$$

In the outward path, the nodes are splitters so the temperature entering the node is equal to the temperature leaving it:

$$T_p(t, x = L_p) = T_{p+1}(t, x = 0) = T_{in_p}(t, x = 0) \quad p = 1 \dots 12, 14 \dots 19$$

$$T_p(t, x = L_p) = T_{in_p}(t, x = 0) \quad p = 13, 20 \tag{4}$$

$$T_0(t, x = L_p) = T_1(t, x = 0,) = T_{14}(t, x = 0)$$

In the return path, the nodes are mixers. We apply an energy balance considering the equality between the inlet and outlet enthalpy flows. Assuming a constant specific heat capacity between the inlet and the outlet, the equation is:

$$\dot{m}_{p_r}(t) \cdot T_{p_r}(t, x = 0) = \dot{m}_{(p+1)_r}(t) \cdot T_{(p+1)_r}(t, x = L_{(p+1)_r}) + \dot{m}_{out_p}(t) T_{out_p}(t, x = L_{out_p}) \quad p = 1 \dots 12, 14 \dots 19$$

$$T_{p_r}(t, x = 0) = T_{out_p}\left(t, x = L_{out_p}\right) \quad p = 13, 20 \tag{5}$$

$$\dot{m}_{0_r}(t) \cdot T_{0_r}(t, x = 0) = \dot{m}_{1_r}(t) \cdot T_{1_r}(t, x = L_{1_r}) + \dot{m}_{14_r}(t) T_{14_r}(t, x = L_{14_r})$$

L, $\dot{m}(t)$ and $T(x,t)$ are the pipe length, mass flow and temperature of water in the pipes. x and t represent the time and distance dependencies.

The sub-station unit is also defined by mass and energy balance equations. The flow going from the outward path to the substation is equal to the flow going from the substation to the return path. Assuming a constant specific heat capacity, the energy balance is defined to have a difference in enthalpy flows between the inlet and the outlet equal to the demand. The conservation equations of the sub-station are:

$$\dot{m}_{in_p}(t) = \dot{m}_{out_p}(t) \quad p = 1 \dots 20 \tag{6}$$

$$Demand(t) = \dot{m}_{in_p}(t) \cdot \mathrm{c}_w \cdot \left[T_{in_p}(t, x = L_{in_p}) - T_{out_p}(t, x = 0)\right] \quad p = 1 \dots 20 \tag{7}$$

c_w is the specific heat capacity of water.

3.2. Thermal model of the pipe

As stated in [17], the choice of an adequate pipeline model that gives a good trade-off between accurate physics and computing costs is a key challenge for DHN optimization. As proposed in previous studies [14,18,19] we use a one-dimensional energy balance in the pipe which is described by the partial differential equation (PDE) written in Eq. (8). This heat transfer equation is submitted to the following assumptions:

- Plug flow
- Neglected axial conductive heat transfer in the fluid
- Material properties are constant and independent of temperature
- Thermal interaction between the supply and return pipes is not included
- Thermal inertia of the pipes, casing and insulation is neglected

$$\rho \cdot c_w \cdot A_k \cdot \frac{\partial T_k(t,x)}{\partial t} + \dot{m}_k(t) \cdot c_w \cdot \frac{\partial T_k(t,x)}{\partial t} = \frac{T_s(t) - T_k(t,x)}{R_k(t)} \tag{8}$$

$$k = \{0, \dots, 20, 0_r, \dots, 20_r, in_1, \dots, in_{20}, out_1, \dots, out_{20}\}$$

ρ and A are the water density and cross section area, respectively. $R(t)$ represents the total dynamic thermal resistance per unit length of pipe and $T_s(t)$ is the temperature of the soil surface.

The total thermal resistance over time $R(t)$ depends on the thermal conductivities of the pipe, insulation, casing and soil. $R(t)$ depends also on the internal convective heat transfer between the water and the inner wall of the pipe and is given by [18]:

$$R_k(t) = \frac{1}{2\pi r_{a_k} \overline{h}_k(t)} + \frac{\ln\left(\frac{r_b}{r_{a_k}}\right)}{2\pi\lambda_{ab}} + \frac{\ln\left(\frac{r_c}{r_b}\right)}{2\pi\lambda_{bc}} + \frac{\ln\left(\frac{r_d}{r_c}\right)}{2\pi\lambda_{cd}} + \frac{1}{S_k \lambda_s} \tag{9}$$

where λ_{ab} , λ_{bc} , λ_{cd} and λ_s represent the thermal conductivities of the pipe, insulation, casing and soil, respectively, and r_a, r_b, r_c and r_d are the different radiuses from the inner wall of the pipe to the casing, as it is shown in Figure 4.

S is the conduction shape factor, for $d > 3r_d$, it can be approximated by [20]:

$$S_k = \frac{2 \cdot \pi \cdot L_k}{\ln\left(\frac{4 \cdot d}{2 \cdot r_d}\right)} \tag{10}$$

where d is the distance between the pipe axis and the soil surface.

https://doi.org/10.52202/069564-0218

$\bar{h}(t)$ is the convective heat transfer coefficient over time averaged for the entire length of the pipe, it is computed by:

$$\overline{h_k}(t) = \frac{\overline{Nu_k}(t) \cdot \lambda_w}{D_{a_k}} \tag{11}$$

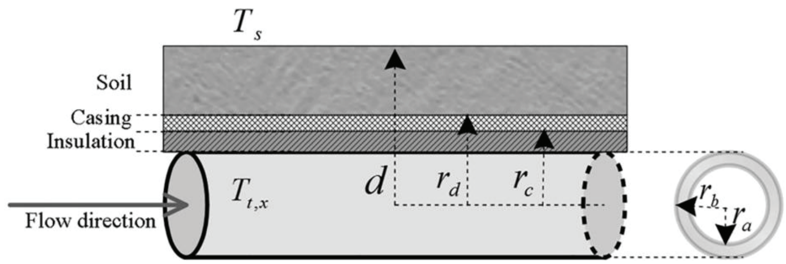

Figure 4. Representation of the buried pipe [15].

where D_a is the pipe internal diameter ($D_a = 2r_a$), $\overline{Nu}(t)$ is the Nusselt number over time averaged for the entire length of the pipe and λ_w is the thermal conductivity of water. Assuming that the system operates under a turbulent regime (Reynolds ≥ 9000), we use the correlation of Dittus-Boelter [21] to compute the Nusselt number in a circular tube:

$$\overline{Nu}_k(t) = 0.023 \cdot (Re_k(t))^{0.8} \cdot Pr^{0.4} \tag{12}$$

$Re(t)$ and Pr are the Reynolds number over time and the Prandtl number, respectively:

$$Re_k(t) = \frac{2 \cdot \rho \cdot v_k(t) \cdot D_{a_k}}{\mu} \tag{13}$$

$$Pr = \frac{\mu \cdot c_w}{\lambda_w} \tag{14}$$

$v(t)$ and μ are the flow velocity over time and dynamic viscosity of water, respectively.

3.3. Hydraulic model of the pipe

The work of the pumps in the distribution network is directly related to the pressure drops. For each pipe, to compute the linear pressure drops, the Darcy-Weisbach equation is used:

$$\Delta P_{linear_k}(t) = f_k(t) \cdot \frac{L_k}{D_{a_k}} \cdot \rho \cdot \frac{[v_k(t)]^2}{2} \quad k = \{0, \dots, 20, 0_r, \dots, 20_r, in_1, \dots, in_{20}, out_1, \dots, out_{20}\} \tag{15}$$

$f(t)$ represents the friction factor over time which depends on the flow regime and the rugosity of the pipe. For $4 \cdot 10^3 \leq Re \leq 10^8$ and a relative roughness ε/D smaller than 10^{-2}, it can be computed by the form of Colebrook-White equation proposed by Moody [22]:

$$f_k(t) = 0.0055 \left\{1 + \left[2 \cdot 10^4 \left(\frac{\varepsilon}{D_{a_k}}\right) + \frac{10^6}{Re_k(t)}\right]^{1/3}\right\} \tag{16}$$

We assume that we have smooth pipes, which means $\varepsilon/D_{a_k} = 0$. The singular pressure drops are assumed to be equal to 30% of the total pressure drops [4]. In each branch, the total pressure drop is equal to the sum of the linear and singular pressure drops. As we have parallel connections, we choose the longest path to compute the linear pressure drops. For the left branch (LB), the pressure drop is:

$$\Delta P_{Total_{LB}}(t) = \frac{1}{0.7} \sum_{k_{LB}} \Delta P_{linear_k}(t) \tag{17}$$

with: $k_{LB} = \{1, \dots, 13, 1_r, \dots, 13_r, in_{13}, out_{13}\}$

For the right branch (RB), the pressure drop is:

$$\Delta P_{Total_{RB}}(t) = \frac{1}{0.7} \sum_{k_{RB}} \Delta P_{linear_k}(t) \tag{18}$$

with: $k_{RB} = \{14, \dots, 20, 14_r, \dots, 20_r, in_{20}, out_{20}\}$

The fact that the LB is longer and serves more consumers than the RB, suggests that the $\Delta P_{Total_{LB}}(t)$ should be higher than the $\Delta P_{Total_{RB}}(t)$. We assume that at every time step, the pressure drop of the LB is higher than the one of the RB. We also neglect the singular pressure drops in the pipes 0 and 0_r. The electrical power required for the pump is:

https://doi.org/10.52202/069564-0218

$$Pw_{pump}(t) = \frac{\dot{m}_0(t)}{\eta\rho}\left[\Delta P_{linear_0}(t) + \Delta P_{linear_{0_r}}(t) + \Delta P_{Total_{LB}}(t)\right] \quad (19)$$

η is the pump efficiency, it represents the total efficiency of the pump which includes mechanical, transmission and motor efficiencies. η is assumed to be equal to 70%.

Depending on the inner diameter of the pipe, a maximum flow velocity is recommended, which limits the specific pressure drop over the pipe length. A threshold of maximum specific pressure drop of 100-150 Pa/m is common to avoid corrosion and increased pumping energy [23]. Using the recommended flow velocities for sizing pipes reported in [24], we imposed an inequality constraint on each pipe to don't exceed a maximum flow velocity per diameter:

$$v_k(t) \leq v_{max_k} \quad (20)$$

We consider that every consumer have to respect a contractual outlet temperature, for this purpose we defined this equality constraint:

$$T_{out_p}(t, x = 0) = constant \quad p = 1 \dots 20 \quad (21)$$

In order to have values that are available in reality, the diameters of the pipes are bounded to a maximum value of 0.57m that is based on the commercial availability of PVC pipes:

$$D_{a_k} \leq 0.57 \quad (22)$$

The set of Eq. (2) to (22) represent the equality and inequality constraints of the optimization problem, resulting in a partial differential algebraic equation (PDAE) system. The orthogonal collocation on finite elements (OCFE) method was used to discretize the PDE (8) in order to transform the PDAE system into a set of algebraic equations. The details of the implementation of the OCFE and the discretized mathematical model of the system are presented in the appendices A and B of [15], respectively.

4. Objective function

The objective function includes the operational expenditures (OPEX) of the system and the capital expenditures (CAPEX) of the pipes. The OPEX comprise both heat production and pumping costs. The heat production cost "$Cost_{prod}$" is obtained by multiplying the total thermal energy produced over the day by the unit cost of heat production:

$$Cost_{prod} = c_{hot} \cdot \int_1^{24} Pw_{hot}(t)\, dt \quad (23)$$

with: $Pw_{hot}(t) = \dot{m}_0(t) \cdot c_w \cdot \left[T_0(t, 0) - T_{0_r}(t, L_{0_r})\right]$ (24)

c_{hot} is the unit cost of heat production, its unity is (€/MWh), $\dot{m}_0(t)$ is the production mass flow (kg/s) and $T_0(t, 0)$ and $T_{0_r}(t, L_{0_r})$ are the production and return temperatures, respectively. The total thermal energy produced is computed by integrating with respect to time the thermal power $Pw_{hot}(t)$ which is equal to the difference between the enthalpy fluxes of production and return.

The pumping cost "$Cost_{pump}$" is the product of the total pumping energy over the day and the unit cost of electricity:

$$Cost_{pump} = c_{elec} \cdot \int_1^{24} Pw_{pump}(t)\, dt \quad (25)$$

c_{elec} represents the unit cost of electricity, its unity is (€/MWh). The pumping power of the network $Pw_{pump}(t)$ is integrated over the day to obtain the total pumping energy. As Gaussian quadrature methods are suited for the computation of integrals when the OCFE is used, for the resolution of the integrals presented in Eq. (23) and Eq. (25) the Gauss-Lobatto quadrature was employed.

The investment cost of the pipes "$Cost_{inves}$" which includes the cost of the pipes and the cost of deploying them in trenches is represented by a linear function as follows:

$$Cost_{inves} = \sum_k L_k \cdot (\alpha D_{a_k} + \beta) \quad (26)$$

Values of investment cost of different nominal diameter by unit length were given by a French company which operates DHN. Using these values, we create a linear regression to have a continuous representation of the cost depending on the diameter. Considering that the DHN of this case study has a lifetime of 30 years, we transform the coefficients of the linear regression (α and β) to have an investment cost for one day.

Using a Lagrange problem type formulation, the objective function is the sum of the three costs defined above:

$$\min_{\substack{D_{a_k} \\ \dot{m}_k(t) \\ T_k(x,t)}} \left(Cost_{prod} + Cost_{pump} + Cost_{inves}\right) \quad (27)$$

https://doi.org/10.52202/069564-0218

The optimization variables are the inner diameters of the pipes, the temporal values of mass flows, and spatio-temporal values of temperature in each pipe. This optimization aims to find the diameters that give the best trade-off between CAPEX and OPEX while finding the optimal operational values of mass flows and temperatures.

Since all the variables are continuous, Eq. from (2) to (26) and the objective function (27) constitute a dynamic NLP problem. The OCFE was employed on the PDE (8) to transform the problem into a set of algebraic equations. For the resolution, we used an equation-oriented (simultaneous) methodology, with the software GAMS for the modeling of the system, and the solver CONOPT for the solving.

As it is the case in most complex optimization problems, a resolution methodology was developed. The purpose of the methodology is to help the solver by creating a resolution process where we solve successive problems. We start from a simple problem and we get more complex until we finally solve the problem of this study. In the resolution process, we always use the last solution for the initial values of variables of the next problem.

5. Results and discussion

This optimization was done considering a production temperature of 92 °C and an outlet temperature of consumers equal to 72 °C. The unit cost of electricity was taken equal to 174 €/MWh. Concerning the unit cost of heat production, we considered the prices in France in 2022 for 3 different technologies: biomass boiler (50 €/MWh), gas boiler (150 €/MWh) and heat recovery (20 €/MWh). The thermo-physical properties of water are taken for the temperatures of 92 °C and 72 °C as it is shown in Table 2. In what follows, we will present some results obtained in the optimization of this case study.

Table 2. Thermophysical properties of water [20].

	ρ (kg/m^3)	c_w (kJ/(kg K))	$\mu \cdot 10^3$ (N s/m^2)	k (W/(m K))
Outward pipes (92 °C)	963.4	4.209	0.306	0.677
Return pipes (72 °C)	976.6	4.191	0.389	0.664

Figure 5 represents the daily evolutions of heat production and mass flow at the production level for the case of biomass boiler. We observe that the heat production has the same profile as the total demand with slightly higher values due to the thermal losses in the network. The thermal losses can also be observed in Figure 6 where the return temperature to the production is represented. The production mass flow of Figure 5 also has the same profile as the total demand. Since production temperature is constant and return temperature does not vary significantly, the mass flow follows the demand as it can be seen in Eq. (7). We obtain the same evolutions for the two other production technologies (gas boiler, heat recovery).

The pressure drops have daily profiles quite similar to the total demand due to the fact that they are proportional to the square of velocity (Figure 7). Inside the pipes, as there is a plug flow regime, the velocity and mass flow have the same profile. As expected, the pressure drop of the left branch is always higher than the one of the right branch which is explained by a more important demand on the left. In a real case, the DHN cannot operate under these pressure conditions. To guarantee a correct operation, it is necessary to have pressure control valves before mixing nodes that will maintain the same pressure drop in every parallel connection of pipes. Consequently, the pressure drop of the right branch will be equal to the one of the left.

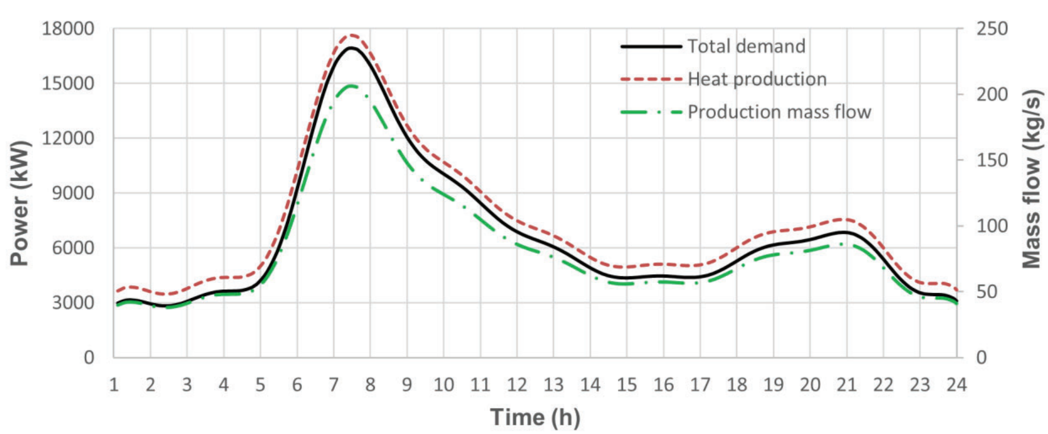

Figure 5. Heat production and production mass flow over time.

https://doi.org/10.52202/069564-0218

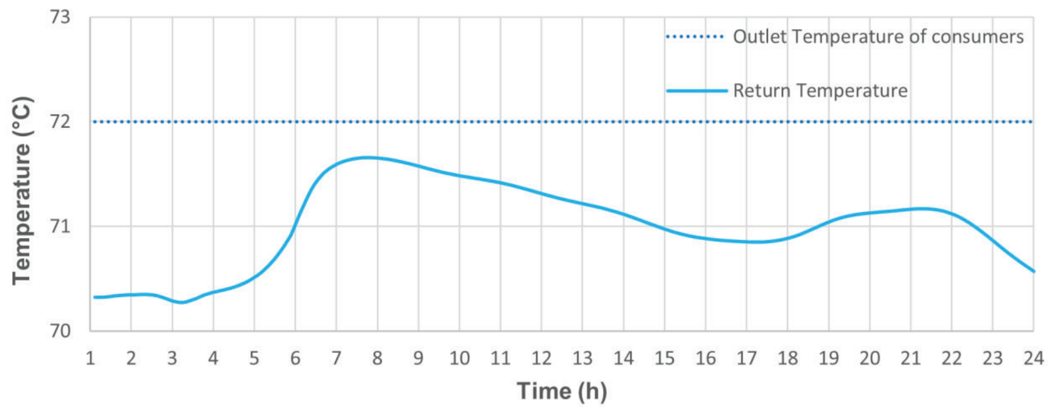

Figure 6. Outlet temperature of consumers and return temperature of the network over time.

In Table 3, we present the results of 3 optimizations where all the parameters are the same (c_{elec}, $Cost_{inves}$, $Demand(t)$, …) except for the unit cost of heat production (c_{hot}). Each unit cost represents a different production technology (gas, biomass and heat recovery). We observe that when c_{hot} increases, the heat produced energy decreases and the pumping energy increases. When the price of heat is more important, the solution tends to reduce the size of the diameters resulting in less investment for pipes, less thermal losses and more pressure drops as it can be observed in Figure 8.

Table 3. Optimization results for 3 different production technologies.

Type of production	Unit cost (€/MWh)	Total heat produced (MWh)	Total pumping energy (kWh)	Average diameter (mm)
Gas boiler	150	169.11	652.82	154.55
Biomass boiler	50	169.17	591.43	155.34
Heat recovery	20	169.20	567.35	155.86

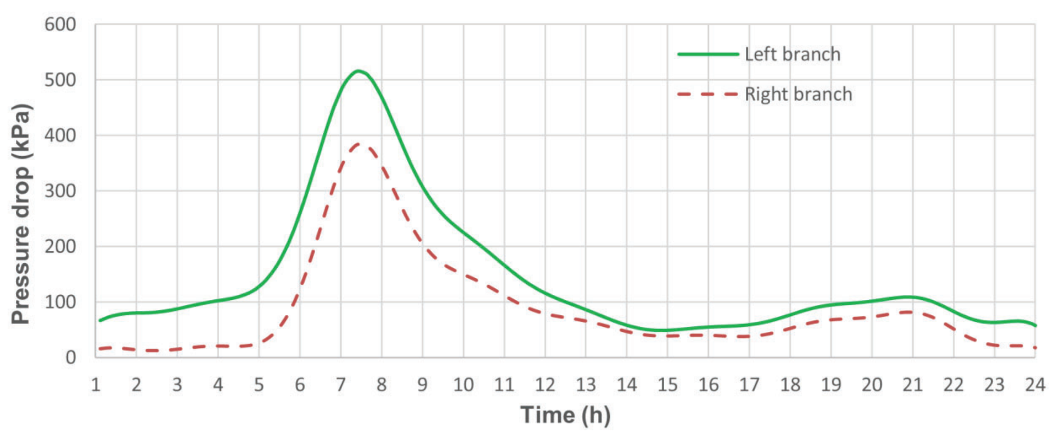

Figure 7. Pressure drops of the two branches of the network over time.

https://doi.org/10.52202/069564-0218

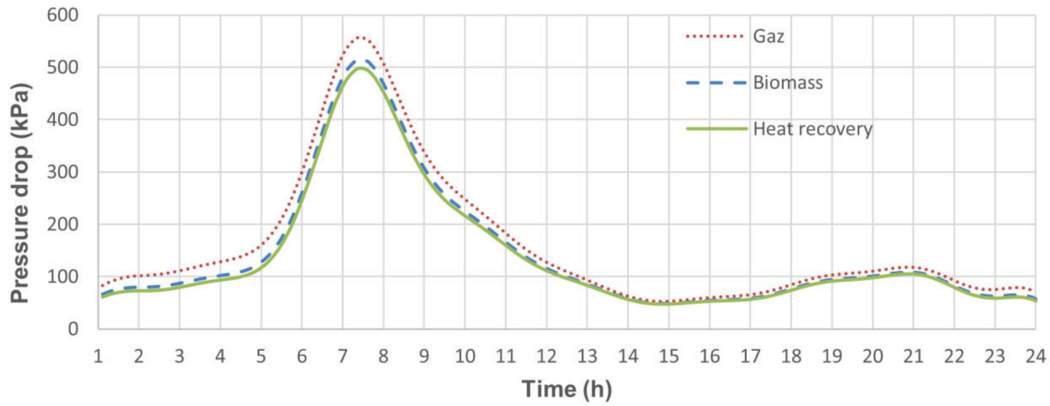

Figure 8. Pressure drop of the left branch of the network for 3 different production technologies.

6. Conclusions and perspectives

In this study, we developed a model for the optimization of the daily operation of a DHN. We optimized the pipe diameters in addition to the mass flows and temperatures in the distribution network. In the modeling of the pipes, the OCFE was used to discretize the heat transfer equation, and the Darcy-Weisbach equation described the pressure drops. The parametric study on the unit cost of heat production confirmed that it is better to have smaller diameters when the cost increases to reduce the thermal losses.

The results of this NLP optimization are a good starting point for a Mixed Integer Dynamic Optimization (MIDO). As we find only discrete values of diameters in the market, it is more interesting to solve a MIDO problem where the diameters will be discrete variables and mass flows and temperatures continuous ones. Moreover, to correctly design the pipes, it is necessary to take into account the operation of the DHN in the different seasons. An interesting study may be the consideration of different characteristic days (one for each season). Another interesting study is the consideration of more than one production unit and of a TES tank. The aim would be to optimize the management of all units while considering the same physical complexity in the pipes and the temperature distribution inside the TES. Currently, we are working on the development and the optimization of a model of this type.

Nomenclature

Abbreviations

CAPEX CAPital EXpenditures
DCN District Cooling Network
DHC District Heating and Cooling
DHN District Heating Network
DOO Dynamic Offline Optimization
MIDO Mixed Integer Dynamic Optimization
MILP Mixed Integer Linear Programming
MINLP Mixed Integer Non-Linear Programming
NLP Non-Linear Programming
OCFE Orthogonal Collocation on Finite Elements
OPEX OPerational EXpenditures
PDAE Partial Differential Algebraic Equation
PDE Partial Differential Equation
TES Thermal Energy Storage

Latin symbols

A cross section area of the pipe, m^2
c_w specific heat capacity of water, J/(kg K)
D pipe diameter, m
f friction factor
L pipe length, m

$\dot{m}$ mass flow in the pipe, kg/s

Pw_{hot} thermal power, W

Pw_{pump} electrical power of the pump, W

r radius, m

R total thermal resistance per unit length of pipe, (m K)/W

Re Reynolds number

t time variable, s

T temperature of the flow in the pipe, °C

v flow velocity, m/s

x space variable, m

Greek symbols

ρ water density, kg/m3

μ dynamic viscosity of water, Pa s

ΔP pressure drops, Pa

λ thermal conductivity, W/(m K)

η pump efficiency

Sets and indexes

a index for the inner diameter of the pipe

C_p set of consumers

k set of pipes

LB index of the left branch of the network

RB index of the right branch of the network

s index for the soil

w index for water

p sub-set for main forward pipes

p_r sub-set for main return pipes

in_p sub-set for pipes entering consumers

out_p sub-set for pipes leaving consumers

References

[1] "Renewable Energy Policies in a Time of Transition: Heating and Cooling – Analysis," *IEA*. https://www.iea.org/reports/renewable-energy-policies-in-a-time-of-transition-heating-and-cooling (accessed Mar. 14, 2023).

[2] M. Vesterlund, A. Toffolo, and J. Dahl, "Optimization of multi-source complex district heating network, a case study," *Energy*, vol. 126, pp. 53–63, May 2017, doi: 10.1016/j.energy.2017.03.018.

[3] R. E. Best, P. Rezazadeh Kalehbasti, and M. D. Lepech, "A novel approach to district heating and cooling network design based on life cycle cost optimization," *Energy*, vol. 194, p. 116837, Mar. 2020, doi: 10.1016/j.energy.2019.116837.

[4] T. Mertz, S. Serra, A. Henon, and J.-M. Reneaume, "A MINLP optimization of the configuration and the design of a district heating network: Academic study cases," *Energy*, vol. 117, pp. 450–464, Dec. 2016, doi: 10.1016/j.energy.2016.07.106.

[5] M. Blommaert, Y. Wack, and M. Baelmans, "An adjoint optimization approach for the topological design of large-scale district heating networks based on nonlinear models," *Applied Energy*, vol. 280, p. 116025, Dec. 2020, doi: 10.1016/j.apenergy.2020.116025.

[6] Y. Liu, H. Tang, Y. Chen, D. Wang, and C. Song, "Optimization of layout and diameter for distributed solar heating network with multi-source and multi-sink," *Energy*, vol. 258, p. 124788, Nov. 2022, doi: 10.1016/j.energy.2022.124788.

[7] M. Sameti and F. Haghighat, "Optimization of 4th generation distributed district heating system: Design and planning of combined heat and power," *Renewable Energy*, vol. 130, pp. 371–387, Jan. 2019, doi: 10.1016/j.renene.2018.06.068.

[8] N. Deng *et al.*, "A MINLP model of optimal scheduling for a district heating and cooling system: A case study of an energy station in Tianjin," *Energy*, vol. 141, pp. 1750–1763, Dec. 2017, doi: 10.1016/j.energy.2017.10.130.

 https://doi.org/10.52202/069564-0218

[9] M. Wirtz, L. Neumaier, P. Remmen, and D. Müller, “Temperature control in 5th generation district heating and cooling networks: An MILP-based operation optimization,” *Applied Energy*, vol. 288, p. 116608, Apr. 2021, doi: 10.1016/j.apenergy.2021.116608.

[10] J. Söderman, “Optimisation of structure and operation of district cooling networks in urban regions,” *Applied Thermal Engineering*, vol. 27, no. 16, pp. 2665–2676, Nov. 2007, doi: 10.1016/j.applthermaleng.2007.05.004.

[11] R. Khir and M. Haouari, “Optimization models for a single-plant District Cooling System,” *European Journal of Operational Research*, vol. 247, no. 2, pp. 648–658, Dec. 2015, doi: 10.1016/j.ejor.2015.05.083.

[12] S. J. Cox, D. Kim, H. Cho, and P. Mago, “Real time optimal control of district cooling system with thermal energy storage using neural networks,” *Applied Energy*, vol. 238, pp. 466–480, Mar. 2019, doi: 10.1016/j.apenergy.2019.01.093.

[13] M. Lu *et al.*, “Operational optimization of district heating system based on an integrated model in TRNSYS,” *Energy and Buildings*, vol. 230, p. 110538, Jan. 2021, doi: 10.1016/j.enbuild.2020.110538.

[14] G. Schweiger, P.-O. Larsson, F. Magnusson, P. Lauenburg, and S. Velut, “District heating and cooling systems – Framework for Modelica-based simulation and dynamic optimization,” *Energy*, vol. 137, pp. 566–578, Oct. 2017, doi: 10.1016/j.energy.2017.05.115.

[15] A. Nova-Rincon, S. Sochard, S. Serra, and J.-M. Reneaume, “Dynamic simulation and optimal operation of district cooling networks via 2D orthogonal collocation,” *Energy Conversion and Management*, vol. 207, p. 112505, Mar. 2020, doi: 10.1016/j.enconman.2020.112505.

[16] I. Petkov and P. Gabrielli, “Power-to-hydrogen as seasonal energy storage: an uncertainty analysis for optimal design of low-carbon multi-energy systems,” *Applied Energy*, vol. 274, p. 115197, Sep. 2020, doi: 10.1016/j.apenergy.2020.115197.

[17] J. Maurer, O. M. Ratzel, A. J. Malan, and S. Hohmann, “Comparison of discrete dynamic pipeline models for operational optimization of District Heating Networks,” *Energy Reports*, vol. 7, pp. 244–253, Oct. 2021, doi: 10.1016/j.egyr.2021.08.150.

[18] J. Duquette, A. Rowe, and P. Wild, “Thermal performance of a steady state physical pipe model for simulating district heating grids with variable flow,” *Applied Energy*, vol. 178, pp. 383–393, Sep. 2016, doi: 10.1016/j.apenergy.2016.06.092.

[19] B. van der Heijde *et al.*, “Dynamic equation-based thermo-hydraulic pipe model for district heating and cooling systems,” *Energy Conversion and Management*, vol. 151, pp. 158–169, Nov. 2017, doi: 10.1016/j.enconman.2017.08.072.

[20] T. L. Bergman, F. P. Incropera, D. P. DeWitt, and A. S. Lavine, *Fundamentals of Heat and Mass Transfer*. John Wiley & Sons, 2011.

[21] R. H. S. Winterton, “Where did the Dittus and Boelter equation come from?,” *International Journal of Heat and Mass Transfer*, vol. 41, no. 4, pp. 809–810, Feb. 1998, doi: 10.1016/S0017-9310(97)00177-4.

[22] L. Zaghadnia, J. L. Robert, and B. Achour, “Explicit solutions for turbulent flow friction factor: A review, assessment and approaches classification,” *Ain Shams Engineering Journal*, vol. 10, no. 1, pp. 243–252, Mar. 2019, doi: 10.1016/j.asej.2018.10.007.

[23] I. Best, J. Orozaliev, and K. Vajen, “Impact of Different Design Guidelines on the Total Distribution Costs of 4th Generation District Heating Networks,” *Energy Procedia*, vol. 149, pp. 151–160, Sep. 2018, doi: 10.1016/j.egypro.2018.08.179.

[24] C. Branan, Ed., *Rules of thumb for chemical engineers: a manual of quick, accurate solutions to everyday process engineering problems*, 3rd ed. Amsterdam ; New York: Gulf Professional Pub, 2002.